electronics

MDPI

Article

A Novel Approach for Adaptive Partial Sliding Mode Controller Design and Tuning in Non-Minimum Phase Switch-Mode Power Supplies

Mahdi Salimi

Faculty of Engineering and Science, University of Greenwich, Kent ME4 4TB, UK; m.salimi@gre.ac.uk

Abstract: In this article, a novel systematic approach is proposed for a partial sliding mode controller (SMC) design and tuning in non-minimum phase switch-mode power supplies (SMPS). To achieve a more simplified controller in comparison with the conventional SMCs, the partial SMC (PSMC) is introduced in this article, which just requires a part of the sliding surface for controller formulation. The accuracy of the developed PSMC is proved mathematically within the entire range of operation. Since the control parameters of the PSMC are not selected by trial and error, it can maintain the stability and robustness of the closed-loop system in a broad operational range. In this regard, and to develop a systematic approach for robust control of SMPS, a constant frequency equivalent SMC is designed using the converter nominal parameters. Then, the extracted controller is combined with an adaptive component to ensure asymptotical stability against load and line changes. Considering the Lyapunov stability criteria for nonlinear systems, it is proved that the presented SPMC can be used for output voltage regulation in both discontinuous and continuous operating modes with zero steady state error. To avoid the trial and error method during the controller tuning and parameters selection, the system characteristic equation is extracted using the Jacobian approach. Considering the roots of the characteristic equation and the stable range of the closed-loop system, the controller parameters are tuned. Furthermore, in addition to simulation, the developed approach is evaluated practically using the TMS3220F2810 digital signal processor. It is shown that the dynamic response of the proposed approach is faster than the standard double-loop SMC during load and line changes. Additionally, it is seen that the developed controller is robust against model changes in both continuous and discontinuous operations.

Keywords: PSMC; controller tuning; robustness; equivalent control; disturbances; asymptotic stability

Citation: Salimi, M. A Novel Approach for Adaptive Partial Sliding Mode Controller Design and Tuning in Non-Minimum Phase Switch-Mode Power Supplies. *Electronics* **2023**, *12*, 1438. https://doi.org/10.3390/electronics12061438

Academic Editor: Junwei Wang

Received: 23 February 2023
Revised: 7 March 2023
Accepted: 14 March 2023
Published: 17 March 2023

1. Introduction

It is well known that direct output control voltage control of switch-mode power supplies (SMPS) in a wide operating range is significantly complicated due to the nonlinear model, as well as the non-minimum phase nature of switching regulators. Moreover, a couple of uncertain parameters, such as input voltage, load resistance, and other model parameters, leads to model deviation from the nominal operating point. Furthermore, in practice, load variations can result in the operating mode changes between continuous and discontinuous conditions, which can complicate controller design tasks more challenging for SMPS. For these reasons and considering the switching nature of DC choppers, the application of the SMC as a robust non-linear controller drew more attention in recent years. For example, maximum power point tracking of the photovoltaic arrays [1], bus regulation in DC micro-grid systems, and feeding constant-power loads [2], sensor less speed control of the permanent magnet DC motors [3], wireless charger for hybrid electric vehicles [4], and emulator design of an electromechanical actuator used in the more electric aircraft [5] are some examples of nonlinear controller design using the SMC.

One of the well-known challenges of SMC design for SMPS is the output voltage error of the controller within the steady state operation [6]. This issue can easily be mitigated by

adding the output voltage error into the final controlling rule. However, such an approach will significantly deteriorate the fast dynamic response of the SMC. In [7], it is tried to obtain a fast dynamic response by elimination of the integral component using an implicit discrete-time terminal SMC. The controller is developed to directly regulate the output voltage of the buck DC-DC converter, which is a minimum phase system from the controller design viewpoint. Hence, such a method cannot maintain closed-loop stability in a wide operating range of non-minimum phase SMPS.

To eliminate system steady state error and also increase controller robustness against model uncertainties, a novel double-integral SMC is presented in [8] for buck DC-DC converters. In contrast to conventional integral-based SMC, it does not require the current signal of the output capacitor, which leads to simplification of the closed-loop system. Hence, the mentioned double-integral SMC can be implemented by using analogue amplifiers. Additionally, its transient response is significantly faster than the standard double-loop approaches in the continuous conduction mode of operation. However, the controller of [8] suffers from a significant overshoot/undershoot during the transients. As the dynamics of the output capacitor are not considered properly during the controller design, its overall performance in a wide operating range, e.g., at discontinuous operation, is questionable in terms of stability and robustness.

In [9], an SMC is designed for maximum power point tracking of the photovoltaic arrays using buck DC-DC converters. The SMC is developed in a way that fewer sensors are required in the closed-loop system. However, due to the pulsating nature of the converter input current, as well as the low voltage of the photovoltaic arrays, the buck DC-DC converter is not an appropriate candidate for photovoltaic systems. Additionally, the controller designed in [9] cannot be applied directly to other non-minimum phase DC-DC converters.

In [10], robust output voltage regulation of the boost DC-DC converter is studied using cascaded SMC and PI controllers. Considering the non-minimum phase nature of the boost converter, the proposed sliding surface in [10] includes both output voltage and inducer current errors. In this regard, the relationship between reference values of the inducer current and output voltage is calculated through the steady state analysis of the converter. However, such an approach is not correct during transient conditions. Additionally, the steady state analysis is carried out by using the ideal model and the effect of the parasitic elements, e.g., the equivalent series resistances of an inductor, output capacitor, and power switch are neglected. Hence, the controller can have a significant steady state error in a broad range of operations, if the role of parasitic resistances is not negligible.

To eliminate output voltage steady state error in non-minimum phase converters, the two-loop controlling approach is a promising method. It includes an external voltage loop, which determines the reference signal for the internal current loop. For example, in the two-loop controller of [11], a linear proportional–integral controller is used for voltage loop implementation and an SMC for the inner current loop. Application of the integrator in the voltage loop can eliminate output voltage steady state error. However, the dynamic response cannot be fast due to successive delays of cascaded controllers.

To improve the response of SMC against uncertainties, it can be combined with adaptive controllers [12]. The adaptive part of the controller is responsible for load estimation and generating the sliding surface. Hence, it can achieve a more robust behaviour during load changes. The controller is designed using the full averaged state space model of the system in continuous conduction mode. For this reason, the final control law is a complex equation and its practical implementation is more challenging, which is a common drawback of adaptive controllers, e.g., adaptive backstepping [13].

In terminal SMC, by using a nonlinear sliding surface, the converter transient response can be improved significantly. However, the response convergence is entirely sensitive to the initial values of state variables. To cope with this issue, the conventional and terminal SMCs were combined using a nonlinear/linear switching function. However, the developed hybrid controller presented in [14] has a variable switching frequency.

Additionally, a systematic method for controller tuning and gains selection is not provided. Furthermore, it can only be applied within the continuous conduction operation.

It should be noted that due to the simplicity of design, as well as ease of practical implementation, the SMC application for closed-loop control of power electronic converters increased sharply in the recent decade. The standard SMC design begins with the definition of a sliding surface, which can be a linear combination of the system error variables. Such a surface divides the phase plane into two separate parts. System response can be directed toward the sliding surface and desired operating point if an appropriate switching state is applied on each side of the sliding surface. In this regard, if the switching frequency is not controlled directly, the chattering issues can deteriorate the controller response.

By defining an adjustable hysteresis band around the sliding surface, one can limit the switching frequency changes within the allowable margin [15]. This approach (hysteresis-base SMC) is an interesting method since the controller does not include a separate controlling gain and the issues associated with its tuning are not observed. On the other hand, to maintain the system stability in a wide operating range against system uncertainties, adjustment of the hysteresis band is a significantly challenging task, because exact values of the input voltage, load resistance, and inductor should be measured directly. Additionally, it does not guarantee the fixed switching frequency operation during the transients.

On the other hand, an equivalent control method is another approach for model-based fixed-frequency SMC design [16]. The duty cycle of equivalent-based SMC is simply obtained by setting the time derivative of the sliding surface to zero. Then, the developed duty cycle is applied through a PWM unit to the power switch. The drawbacks of equivalent-based SMC can be summarised as:

1. The control rule includes a couple of gains. Hence, if the SMC is tuned by trial and error, its superior performance cannot be guaranteed in a wide range of changes in terms of closed-loop stability and robustness.
2. If the dynamics of all state variables are used in the sliding surface, the final control law can be a complex function in SMPS. For this reason, the practical implementation of the SMC is not straightforward. Moreover, SMC combination with adaptive controllers (although it improves the controller's stability against uncertainties), requires more time-consuming real-time calculations.

To cope with mentioned issues, a novel PSMC is developed for non-minimum phase SMPS. The design includes a systematic approach for both control extraction and gains selection. The proposed controller is developed just by using a part of the sliding surface, which can result in the significant simplification of the final control law. Such an approach leads to the introduction of partial SMC as a simplified fixed-frequency sliding mode controller in this article. The effectiveness of the designed PSMC is proved mathematically within the entire range of operation using the Lyapunov criteria. It should be noted that due to the systematic selection of the controller's gains and avoiding the trial and error method, the controller can maintain the stability and robustness of the closed-loop system in a broad operational range. To provide a systematic method for robust control of non-minimum phase SMPS, first, a constant frequency equivalent SMC is designed using the converter nominal parameters. Then, the extracted controller is combined with an adaptive component to ensure asymptotical stability against load and line changes. Using the Lyapunov stability method, it is shown that the designed PSMC can be successfully used for output voltage regulation in both discontinuous and continuous operating modes with zero steady state error. In addition to simulation results, the controller is implemented practically using the TMS3220F2810 digital signal processor from Texas Instruments for experimental verifications. It is proved that the dynamic response of the proposed approach is faster than the standard double-loop SMC during load and line changes. Additionally, it is seen that the developed controller is robust against model changes in both continuous and discontinuous operations.

2. Conventional SMC Design

In this section, the averaged state space modelling of the SMPS, e.g., buck/boost DC-DC converter and its non-minimum behaviour during direct output voltage control is reviewed. Additionally, the application of cascaded two-loop controllers and their different implementation methods are introduced. Finally, another SMC and how the outer and inner loops can be merged are explained. Such an approach mitigates the issues of standard two-loop controllers in terms of loop delays.

2.1. Non-Minimum Phase Nature of the Converter

According to Figure 1, the converter-averaged state space model in both discontinuous and continuous modes can be written as [17]:

$$\begin{cases} \dot{x}_1 = -\frac{1}{L}(1-u)x_2 + \frac{\Delta}{L}x_2 + \frac{V_i}{L}u - \frac{r_L}{L}(1-\Delta)x_1 \\ \dot{x}_2 = \frac{1}{C}(1-u)x_1 - \frac{\Delta}{C}x_1 - \frac{1}{RC}x_2 \end{cases} \tag{1}$$

where u is the system control input (duty cycle). Obviously, in continuous operation, the value of Δ is zero. In discontinuous operation, the value of this parameter depends on the load resistance, inductor value, and switching frequency. Assuming $u = D + d$ and neglecting r_L, small-signal transfer functions of the converter in continuous mode can be obtained where D is the converter duty cycle and d indicates its small-signal changes.

$$H_V(s) = \frac{v_o}{d} = \frac{V_i\left(R - sLD/(1-D)^2\right)}{s^2LRC + sL + R(1-D)^2} \tag{2}$$

$$H_I(s) = \frac{i_o}{d} = \frac{V_i(1 + D + sRC/(1-D)}{s^2LRC + sL + R(1-D)^2} \tag{3}$$

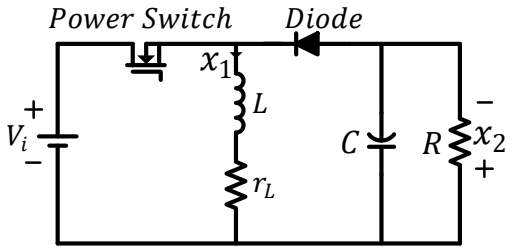

Figure 1. Buck/boost DC-DC converter and inducer current waveform in discontinuous conduction mode. The value of Δ is zero in continuous operating mode.

2.2. Output Voltage Indirect Control

Considering the presence of a right half plane zero in (2), clearly the $H_V(s) = \frac{v_o}{d}$ is a non-minimum phase system and hence, the stability of the closed-loop system cannot be maintained in a wide operating range if an output voltage direct controller is used. However, such an issue is not observed within the inductor current control. By setting the state variables derivatives zero in (1):

$$I_L = \left(1 + \frac{V_o}{V_i}\right)\left(\frac{V_o}{R}\right) \tag{4}$$

where I_L and V_o are inductor current and output voltage, respectively, in steady state operation. Equation (4) indicates that there is a direct relationship between system state variables. Hence, the output voltage can be controlled indirectly by adjusting the inductor current using the block diagram illustrated in Figure 2a. However:

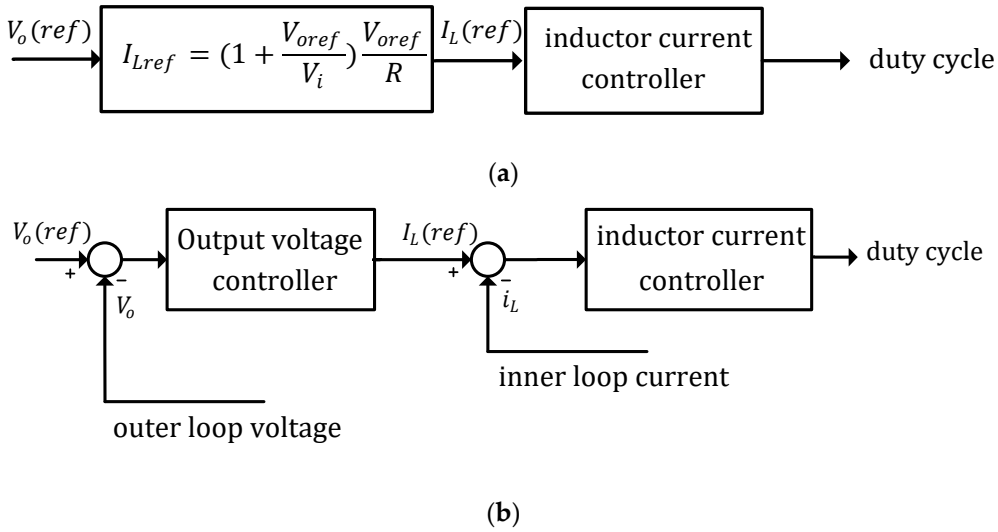

Figure 2. Indirect control of the output voltage. (**a**) Indirect control of the output voltage in non-minimum SMPS. (**b**) Two-loop control of the non-minimum phase SMPS.

(a) Equation (4) is only valid during the steady state operation and it cannot be applied at transients;
(b) Since an ideal model of the converter is used for the formulation of Equation (4), it can lead to a significant error if model non-idealities play an important role at a specific operating point (e.g., while the load resistance is as small as the inductor series resistance);
(c) Since the values of R and V_i are uncertain in (4), extra sensors and units are required for the estimation of mentioned uncertainties.

To overcome these issues, a two-loop control approach, as shown in Figure 2b, can be used. In this method, the external control loop determines a reference signal for the inductor current. Direct feedback of the output voltage in addition to using a PI controller in the external loop can remove the steady sate error efficiently, despite the model uncertainties.

2.3. Implementation of the Two-Loop Controller

Different approaches can be used for the implementation of two-loop controllers, shown in Figure 2b.

Cascade linear controllers: Both controllers of the internal and external loops can be implemented using PI-type linear controllers. However, a PI controller cannot stabilize the SMPS in a wide range due to the nonlinear nature of DC-DC converters.

Combined nonlinear/linear controllers: Nonlinear controllers, such as SMC are employed for the implementation of the internal current loop. However, the external loop is designed based on a linear controller, and as a result, despite some improvements in the performance of the internal loop, the stability of the whole system cannot be guaranteed in a wide range of changes.

Cascade nonlinear controllers: Generally, both loops in Figure 2b can be implemented using nonlinear controllers. However, such an idea is not a promising approach if the SMC is selected as a nonlinear controller due to the switching nature and chattering issues of SMC. In other words, a proper smooth reference current cannot be generated for the internal loop using an SMC in the voltage loop.

2.4. A Unified Single-Loop Indirect Controller

In addition to the mentioned disadvantages of a two-loop controller, it suffers from a slow transient response due to the application of cascaded controlling loops. During the transients, the response of the internal loop will postpone until the steady state operation

of the external loop and completion of reference current generation. To cope with this problem, a unified single-loop SMC can be employed for indirect control of the output voltage in SMPS where separate controlling loops are not required.

It should be noted that the unified single-loop SMC design is a straightforward task. At first, the inducer reference current is defined.

$$i_{Lref} = k_P\Big(V_{ref} - x_2\Big) + k_I \int \Big(V_{ref} - x_2\Big)dt \tag{5}$$

So, the error variables are introduced.

$$\begin{array}{c} z_1 = i_{ref} - x_1 \\ z_2 = V_{ref} - x_2 \\ z_3 = \int (z_1 + z_2)dt \end{array} \tag{6}$$

Defining the sliding surface as $S(z) = \alpha_1 z_1 + \alpha_2 z_2 + \alpha_3 z_3$, equivalent SMC can be obtained using $\dot{S}(z) = \frac{dz}{dt} = 0$ and Equations (1), (5), and (6).

$$\begin{array}{c} u_{eq} = \left[\frac{-1}{(\alpha_1 k_P/C)x_1 + (-\alpha_1/L + \alpha_2/C)x_2 - \alpha_1 V_{in}/L}\right] \times \left\{\left[\frac{\alpha_1 k_P(-1+\Delta)}{C} + \frac{\alpha_2 \Delta}{C} - \alpha_3\right]x_1 + \right. \\ \left[\alpha_1\left(\frac{k_P}{RC} + \frac{(1-\Delta)}{L}\right) + \alpha_2\left(-\frac{1}{C} + \frac{1}{RC}\right)\right]x_2 + [\alpha_1 k_I + \alpha_3(k_P + 1)]\Big(V_{ref} - x_2\Big) + \\ \left. \alpha_3 k_I \int \Big(V_{ref} - x_2\Big)dt\right\} \end{array} \tag{7}$$

Although the unified single-loop SMC expressed in Equation (7) can stabilize the SMPS in a wide operating range in both continuous and discontinuous modes, its drawbacks can be summarised as follows.

a. The values of both Δ and V_i in the mentioned SMC are uncertain;
b. The controller implementation is not straightforward due to the complexity of the control rule;
c. A proper method for selection of the controller gains, including α_1, α_2, α_3, k_p, and k_I, should be addressed. If these parameters are selected by trial and error, it does not guarantee the optimum operation of the system in a wide range.

To cope with these issues, a novel approach for partial SMC design and tuning is presented in this article.

3. Novel Adaptive Partial SMC Design and Tuning

In this section, a novel simplified adaptive partial SMC (PSMC) is introduced for closed-loop control of the SMPS in both continuous and discontinuous operations. At first, considering the model uncertainty, the general model of the non-minimum phase SMPS is rewritten. Then, the PSMC is presented for output voltage regulation. To ensure the stability of the closed-loop system, controller gains are determined by extracting the system characteristic equation and using the roots locus analysis. Finally, the presented PSMC is modified to improve the robustness of the controller against the model uncertainty and also during the mode changes between the discontinuous and continuous operations. The asymptotical stability of the adaptive PSMC is proved using the Lyapunov stability criteria.

3.1. Equivalent PSMC Design

In general form, the converter averaged state space model can be rewritten as:

$$\begin{cases} \dot{x}_1 = -\theta_1(1-u)x_2 + \theta_2 x_2 + \theta_3 u - \theta_7 x_1 \\ \dot{x}_2 = \theta_4(1-u)x_1 - \theta_5 x_1 - \theta_6 x_2 \end{cases} \tag{8}$$

where $\theta_1 = \frac{1}{L}$, $\theta_2 = \frac{\Delta}{L}$, $\theta_3 = \frac{V_i}{L}$, $\theta_4 = \frac{1}{C}$, $\theta_5 = \frac{\Delta}{C}$, $\theta_6 = \frac{1}{RC}$, and $\theta_7 = \frac{r_L}{L}(1-\Delta)$. It should be noted that the nominal and real values of these parameters might be different. So, parameter nominal values can be defined in continuous operating mode as follows:

$$\begin{gathered}\theta_{1n} = \frac{1}{L_n}\ ,\ \theta_{2n} = 0\ , \theta_{3n} = \left(\frac{V_i}{L}\right)_n = \frac{V_{in}}{L_n},\ \theta_{4n} = \frac{1}{C_n}\ ,\ \theta_{5n} = 0\ , \\ \theta_{6n} = \left(\frac{1}{RC}\right)_n = \frac{1}{R_n C_n}\ , \theta_{7n} = 0.\end{gathered} \tag{9}$$

In this regard, δ_i is defined as the difference between the nominal and real values of the i-th parameter.

$$\theta_i = \theta_{in} + \delta_i \qquad (for \quad i = 1\ to\ 7) \tag{10}$$

By replacing (9) and (10) in the system model in (8)

$$\begin{cases}\dot{x}_1 = -\theta_{1n}(1-u)x_2 + \theta_{3n}u + w_1 \\ \dot{x}_2 = \theta_{4n}(1-u)x_1 - \theta_{6n}x_2 + w_2\end{cases} \tag{11}$$

where model uncertain functions, w_1 and w_2 can be expressed as follows:

$$\begin{cases}w_1 = -\delta_1(1-u)x_2 + \delta_2 x_2 + \delta_3 u - \delta_7 x_1 \\ w_2 = \delta_4(1-u)x_1 - \delta_5 x_1 - \delta_6 x_2\end{cases}. \tag{12}$$

Assuming that all parameters are bounded, it can be concluded that w_1 and w_2 are bounded functions as well.

To design the PSMC, system error variables are defined first.

$$\begin{gathered}z_1 = I_{Lref} - x_1 \\ z_2 = V_{ref} - x_2\end{gathered} \tag{13}$$

To eliminate the output voltage error of the controller, the inducer reference current can be defined as follows:

$$I_{Lref} = k_I \int z_2 dt \tag{14}$$

The equivalent controller is designed based on the nominal values of the model parameters in (11) and the controller will be modified in the next sessions to cope with the model.

So, neglecting the bounded uncertain functions, the model can be simplified as follows:

$$\begin{cases}\dot{x}_1 = -\theta_{1n}(1-u)x_2 + \theta_{3n}u \\ \dot{x}_2 = \theta_{4n}(1-u)x_1 - \theta_{6n}x_2\end{cases}. \tag{15}$$

Sliding surface can be defined as:

$$S = z_1 + z_2 + k\int (z_1 + z_2)dt \tag{16}$$

where k is a positive scalar. If it is assumed that the converter dynamics are settled on the sliding surface, then $S = 0$ is obtained. As a result in sliding mode, the time derivative of the sliding surface will be zero as well.

$$\dot{S} = 0 \rightarrow \dot{z}_1 + \dot{z}_2 + k(z_1 + z_2) = 0 \tag{17}$$

Or

$$\dot{S} = M + N = 0 \tag{18}$$

where

$$\begin{gathered}M = \left(\dot{z}_2 + kz_2\right) \\ N = \left(\dot{z}_1 + kz_1\right).\end{gathered} \tag{19}$$

Considering Equations (13) and (14), N can be written as follows:

$$N = k_I\, z_2 - \dot{x}_1 + kz_1. \tag{20}$$

Considering parameters nominal values and using (15), equivalent partial SMC can be obtained by setting Equation (20) to zero.

$$u_{eq} = \frac{1}{\theta_{1n}x_2 + \theta_{3n}}\left(\theta_{1n}x_2 + kz_1 + k_I\, z_2\right) \tag{21}$$

In the next section, it will be proved that the next part of the sliding surface (function M) will also be zero under the designed PSMC. Such an idea results in a simpler SMC because only part (not the whole) of the sliding surface is used for SMC design. By setting error variables to zero in Equation (21), the following equation can be obtained for the steady state operation, which is a well-known formula in buck/boost DC-DC converters:

$$\frac{V_o}{V_i} = \frac{D}{1-D}. \tag{22}$$

3.2. PSMC Tuning

In this section, the controller tuning and gains selection processes (k and k_I) are studied. Assuming $\alpha_n = \frac{\theta_{3n}}{\theta_{1n}}$, $k_1 = \frac{k}{\theta_{1n}}$, and $k_2 = \frac{k_I}{\theta_{1n}}$, the PSMC controller in (21) can be rewritten as:

$$u_{eq} = \frac{1}{x_2 + \alpha_n}\left(x_2 + k_1 z_1 + k_2\, z_2\right). \tag{23}$$

By placing (23) in (15) and using Equation (13), the following closed-loop model can be obtained:

$$\begin{cases} \dot{x}_1 = \theta_{1n}\Big[k_1\Big(I_{Lref} - x_1\Big) + k_2\Big(V_{ref} - x_2\Big)\Big] \\ \dot{x}_2 = \theta_{4n}x_1 - \theta_{6n}x_2 - \frac{\theta_{4n}x_1}{x_2+\alpha_n}\Big[x_2 + k_1\Big(I_{Lref} - x_1\Big) + k_2\Big(V_{ref} - x_2\Big)\Big] \end{cases}. \tag{24}$$

Simply by setting Equation (24) to zero, the steady state operating point of the converter can be obtained as $(X_{1S}, X_{2S}) = \Big(I_{Lref}, V_{ref}\Big)$, where $I_{Lref} = \frac{V_{ref}}{R}\Big(1 + \frac{V_{ref}}{V_i}\Big)$.

According to Jacobin's linearization approach and assuming small-signal changes in the state variable $(\widetilde{x}_1, \widetilde{x}_2)$, a non-linear system can be linearised around an operating point. Considering the model of a nonlinear system as

$$\begin{cases} \dot{x}_1 = f_1(x_1, x_2) \\ \dot{x}_2 = f_2(x_1, x_2) \end{cases} \tag{25}$$

and assuming $x_1 = X_{1S} + \widetilde{x}_1$ and $x_2 = X_{2S} + \widetilde{x}_2$, the linearised model of (25) can be written as follows:

$$\Big(\dot{\widetilde{x}}_1, \dot{\widetilde{x}}_2\Big)^T = J(\widetilde{x}_1, \widetilde{x}_2)^T \tag{26}$$

where J is a 2×2 square matrix which is called a Jacobin matrix. Different arrays of the Jacobin matrix can be calculated as follows:

$$a_{ij} = \left.\frac{\partial f_i}{\partial x_j}\right|_{operating\ point} \qquad (for\ i, j = 1, 2). \tag{27}$$

Considering the system model in (24), the Jacobian matrix can be calculated.

$$\begin{cases} a_{11} = -k_1\theta_{1n} \\ a_{12} = -k_2\theta_{1n} \\ a_{21} = \theta_{4n} + \frac{k_1\theta_{4n}I_{ref} - \theta_{4n}V_{ref}}{V_{ref} + \alpha_n} \\ a_{22} = -\theta_{6n} + \frac{\theta_{4n}I_{Lref}(k_2 - 1)}{V_{ref} + \alpha_n} + \frac{\theta_{4n}I_{Lref}V_{ref}}{(V_{ref} + \alpha_n)^2} \end{cases} \quad (28)$$

In this regard, the nominal values of the converter parameters are listed in Table 1.

Table 1. Nominal parameters of the buck/boost DC-DC converter.

Parameter	Symbol	Value
Input voltage	V_i	12 V
Inducer	L	550 µH
Output capacitor	C	330 µF
Load resistance	R	8.5 Ω

Assuming $V_{ref} = 5$ V, converter reference current can be calculated using (4), which results in $I_{ref} = 0.83$ A. Considering (28), the Jacobin matrix can be obtained using nominal parameters.

$$J = \begin{bmatrix} -k & -k_I \\ 0.08k + 2140 & 0.08k_I - 460.9 \end{bmatrix} \quad (29)$$

System characteristic equation for the designed controller can be calculated using $|sI - J| = 0$ where s is the Laplace operator.

$$s^2 + (460.9 + k - 0.08k_I)s + 460.9k + 2140k_I = 0 \quad (30)$$

Considering the stability theory, the roots of Equation (30) should be in the left half plane. In Figure 3, changes in the characteristic equation roots are illustrated for different gains. It is observed that for $k = 200$, a stable range of the designed controller is obtained as $0 \leq k_i \leq 8100$.

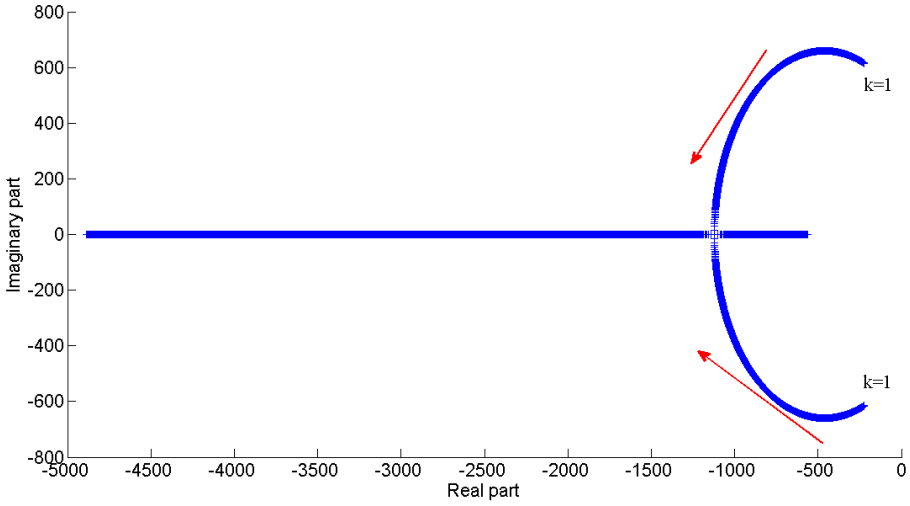

(**a**)

Figure 3. Characteristic equation roots and output voltage of the closed-loop controller for different controller gains. (**a**) Characteristic equation roots during charges of k ($k_I = 200$); (**b**) characteristic equation roots during charges of k_I ($k = 200$); and (**c**) step response of proposed PSMC for different values of k_I at the start−up moment.

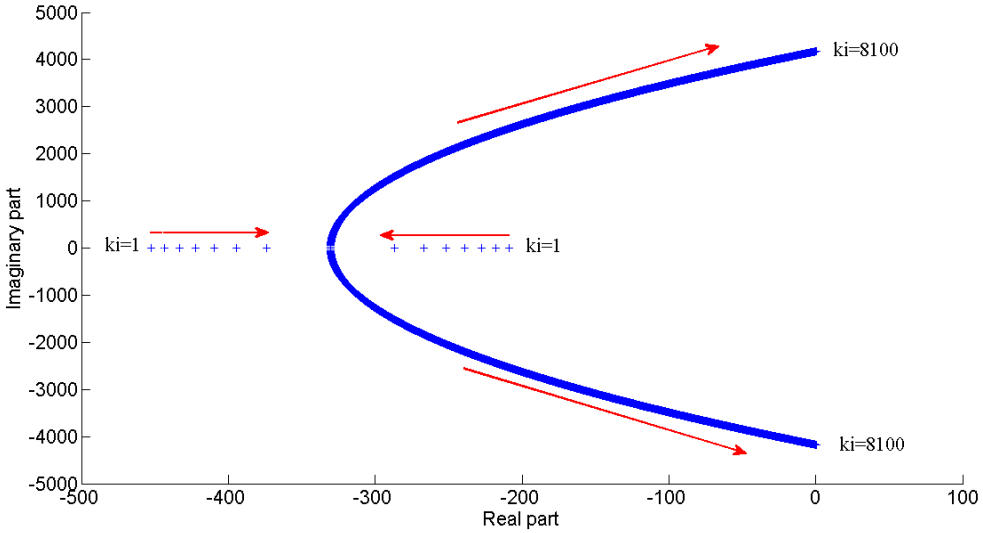

(**b**)

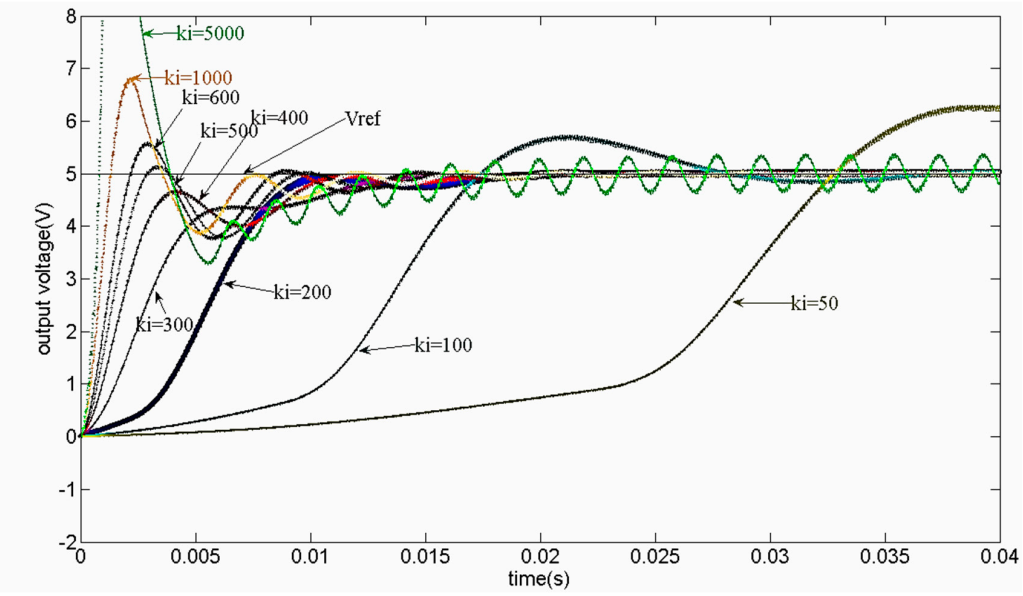

(**c**)

Figure 3. *Cont.*

3.3. Modification of the Designed Controller: Adaptive PSMC

Considering the uncertainties of the converter model in Equation (11), the designed PSMC in (21) is modified in a way that more robust behaviour can be obtained from the developed closed-loop system. If the model's actual parameters are not equal to the nominal values, then $\dot{S} \neq 0$ and the system response will not be settled on the sliding surface. Considering Equations (11), (17), and (20), the sliding surface derivative can be written as:

$$\dot{S} = \dot{S}_n + q \tag{31}$$

$$\dot{S}_n = k_I z_2 + k z_1 + \theta_{1n}(1-u)x_2 - \theta_{3n}u \tag{32}$$

$$q = \dot{z}_2 + k z_2 + \delta_1(1-u)x_2 - \delta_2 x_2 - \delta_3 u + \delta_7 x_1 \tag{33}$$

where S_n is the nominal sliding surface. So, on the sliding surface $S = S_n = 0$. All of the system uncertainties are expressed by q in (31).

In this article, a novel modified PSMC is presented considering system uncertainties as follows:

$$u = u_{eq} + \widetilde{u} = \frac{1}{\theta_{1n}x_2 + \theta_{3n}}[\theta_{1n}x_2 + kz_1 + k_I z_2 + k_C S + \hat{\rho} sgn(S)] \tag{34}$$

where u_{eq} is the system equivalent controller for (35) nominal parameters.

Hence, the controller gains should be selected in a way that $0 \leq u \leq 1$. Additionally, k_C is a positive scalar. In (34), the term $k_C S$ modifies the reaching path of the controller toward the sliding surface. Furthermore, the parameter $\hat{\rho}$ is an estimation from the highest value of system compressed uncertainty function q:

$$|q| < \hat{\rho} \tag{35}$$

Despite the model uncertainties and load disturbances, it can be proved that the system response will place on the sliding surface using the modified controller in (34). In this regard, $\dot{S}$ can be simplified by replacing (34) in (31) and (32).

$$\dot{S} = -[k_C S + \hat{\rho} sgn(S)] + q \tag{36}$$

If the Lyapunov function is defined as

$$V = \frac{1}{2}S^2 + \frac{1}{2}\widetilde{\rho}^2 \tag{37}$$

where $\widetilde{\rho} = \hat{\rho} - \rho$, then the time derivative of the Lyapunov function will be

$$\dot{V} = S\dot{S} + \widetilde{\rho}\dot{\widetilde{\rho}}. \tag{38}$$

By placing (36) in (38) and also considering $\dot{\widetilde{\rho}} = \dot{\hat{\rho}}$, the derivative of the Lyapunov function can be simplified.

$$\dot{V} = S\{-[k_C S + \hat{\rho} sgn(S)] + q\} + \dot{\hat{\rho}}(\hat{\rho} - \rho) \tag{39}$$

Assuming $\dot{\hat{\rho}} = |S|$ and $S \times sgn(S) = |S|$, the Equation (39) can be rewritten as

$$\dot{V} = -k_C S^2 + qS - \rho|S|. \tag{40}$$

It is clear that $qS \leq |q||S|$.

Hence, the following equation can be obtained:

$$\dot{V} \leq -k_C S^2 + |S|(|q| - \hat{\rho}). \tag{41}$$

Since the term $-k_C S^2$ is not a positive expression, and also assuming $|q| < \rho$ in (35), the Lyapunov function derivative will be a negative semi-definite function. So, asymptotical stability of the system will be proved using the developed adaptive PSMC in (34) and the estimation law as $\dot{\hat{\rho}} = |S|$.

3.4. Another Approach for Modification of the PSMC

To improve the system's robustness, an adaptive PSMC is presented in the last section and the estimation law is extracted. According to (42), it can be shown that if $|q|$ is a bounded parameter, asymptotical convergence of the proposed controller can be proved

just by choosing $\rho > |q|$, despite the model uncertainty. In such a way, the estimation rule will no longer be needed.

$$u = \frac{1}{\theta_{1n}x_2 + \theta_{3n}}[\theta_{1n}x_2 + kz_1 + k_Iz_2 + \rho sgn(S)] \tag{42}$$

By replacing the modified controller of (42) in the (31) and (32), the time derivative of the sliding surface can be obtained.

$$\dot{S} = -\rho sgn(S) + q \tag{43}$$

Assuming the Lyapunov function and its time derivative as

$$V = \frac{1}{2}S^2 \rightarrow \dot{V} = S\dot{S} \tag{44}$$

and by replacing $\dot{S}$ from (43) in (44)

$$\dot{V} = S(-\rho sgn(S) + q) = -\rho|S| + qS. \tag{45}$$

Considering $qS \leq |q||S|$, Equation (45) can be simplified as

$$\dot{V} = -\rho|S| + qS \leq -\rho|S| + |q||S|. \tag{46}$$

Hence, if the parameter ρ is selected to meet the condition $\rho > |q|$

$$\dot{V} \leq |S|(-\rho + |q|) \leq 0. \tag{47}$$

Hence, despite the model uncertainties, it is observed that $\dot{V}$ is a negative semi-definite function, which proves the asymptotic stability of simplified PSMC in (42).

4. Simulation and Practical Results

Considering the proposed adaptive PSMC in (42) and parameter nominal values in Table 1, the buck/boost DC-DC converter as a non-minimum phase SMPS is simulated using MATLAB software in different operating points in both continuous and discontinuous operations. Additionally, some experimental tests are carried out by the practical implementation of the controller using TMS320F2910 DSP from Texas Instruments. The inducer current and output voltage of the converter are measured using an isolated Hall effect sensor and IL300-integrated circuit, respectively. Converter switching and sampling frequencies are around 10 kHz and 150 kHz, respectively. The implemented experimental setup is shown in Figure 4.

To evaluate the response of the controller in different operating points, stepped changes in both input voltages and load resistance can be applied by switching the power MOSFETs Q_1 and Q_2 in Figure 4b.

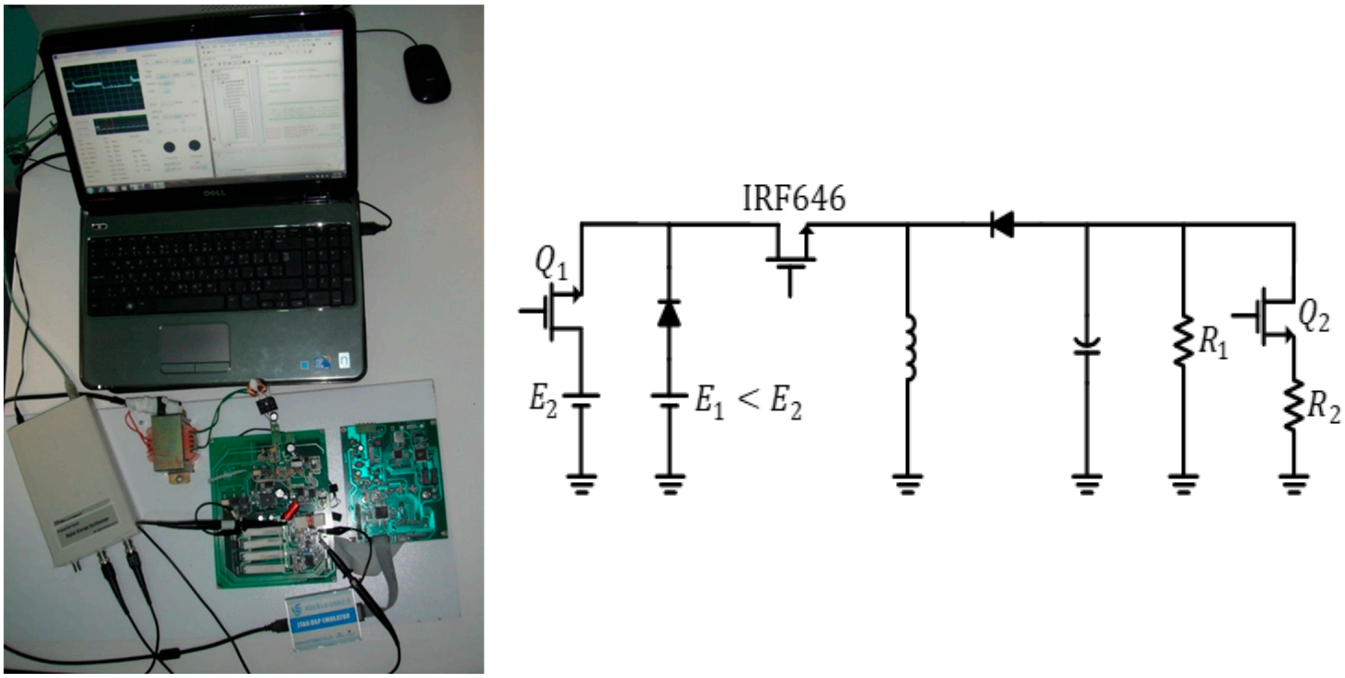

(a) **(b)**

Figure 4. The implemented power circuit. (**a**) The implemented converter. (**b**) Buck/boost DC-DC converter.

4.1. Response of the Proposed Controller Based on Different Controller Gains at Start-Up

As it is shown in Section 2.3, the designed controller is stable for $k = 200$ and $0 \leq k_I \leq 8100$. Assuming $k = 200$, the response of the proposed controller is illustrated for different values of k_I in Figure 3c at the system start-up moment for nominal parameters. It is assumed that the output reference voltage is $V_{ref} = 5$ V. According to Figure 3c, it is clear that the controller has a stable response for $k = k_I = 200$. Hence, all results are obtained based on these gains in the next tests.

4.2. Comparison of the Proposed Controller Response with Standard Two-Loop SMC

To verify the performance of the proposed adaptive PSMC, it is compared with the standard two-loop SMC in [18]. Considering $V_{ref} = 5$ V and converter nominal parameters, the responses of both controllers are presented in Figure 5 at start-up. It is observed that both controllers have stable dynamic responses with zero steady state error.

Additionally, dynamic responses of both SMCs are shown in Figure 5b during step changes of the load resistance in continuous operation where load resistance is changed from nominal value (8.5 Ω) to 8.5‖8.5 Ω at $t = 0.1$ s. It is seen that the proposed adaptive PSMC has a faster dynamic response compared to the standard double-loop SMC.

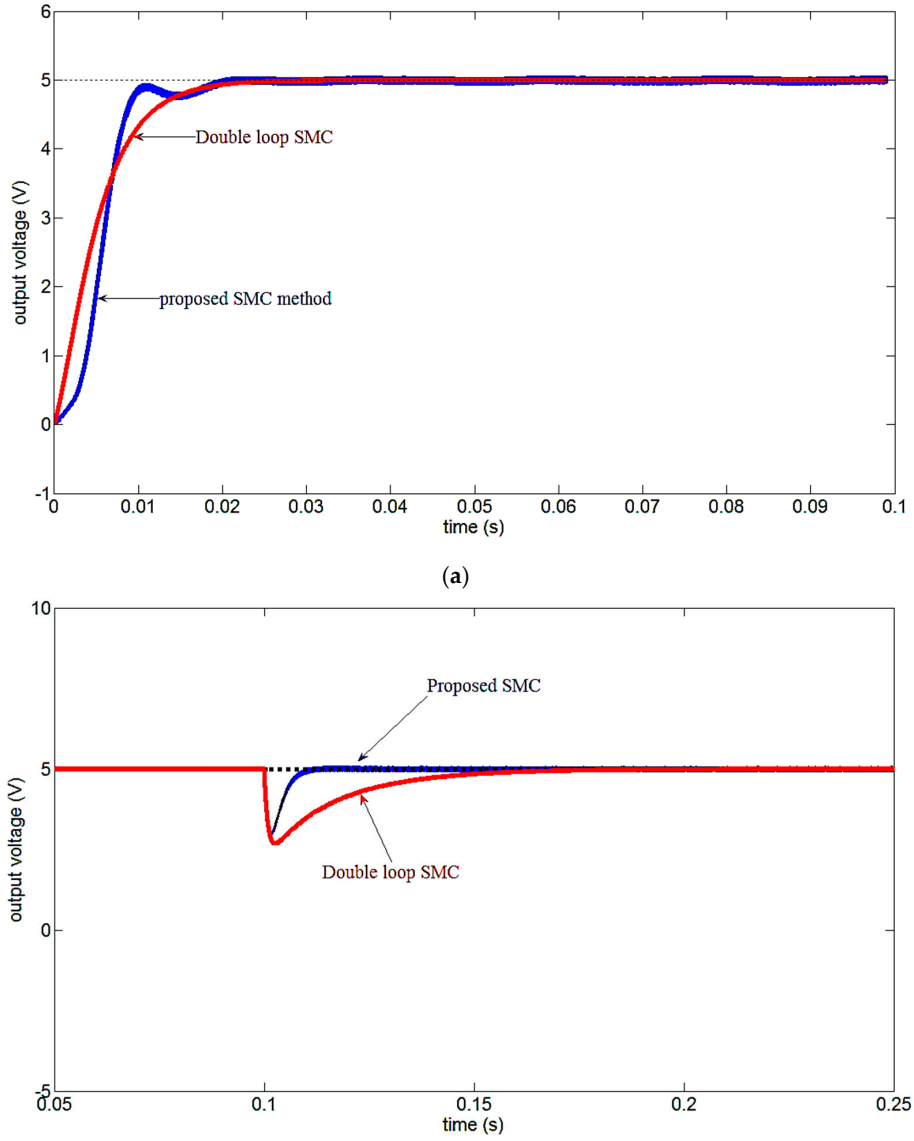

Figure 5. Response of the presented adaptive PSMC in comparison with the standard double-loop SMC2. (**a**) Comparison of the proposed PSMC and double−loop SMC [18] at system start-up. (**b**) Comparison of the proposed adaptive PSMC and double−loop SMC during the converter load changes in continuous operation.

4.3. Experimental Results

Simulation results of the proposed adaptive PSMC are illustrated in continuous operation in Figures 3c and 5. To evaluate the controller in a broader range of operations, the experimental responses are presented considering load and input voltage uncertainties in both discontinuous and continuous modes.

4.3.1. Experimental Response of the Proposed Controller during Load Changes

In Figure 6, the output voltage and inducer current waveforms are illustrated during the step changes of load resistance in a very wide operating range from 200 Ω to 8.5 Ω. Considering the nominal parameters listed in Table 1, it is observed that the converter enters the discontinuous mode, while the load resistance is 200 Ω. So in this experiment, the controller stability at the mode transition moment between continuous and discontinuous operations is investigated.

It is assumed that the reference value of output voltage is +5 V. Despite very large changes in the value of load resistance, it is seen that the proposed controller enjoys a stable and robust performance. Moreover, the steady state error is zero in different operating points.

Finally, the response of standard double-loop SMC [11] is presented in Figure 6a,c in a similar condition. It is observed that the presented adaptive PSMC has a superior performance in terms of fast dynamic response and less overshoot during the load changes.

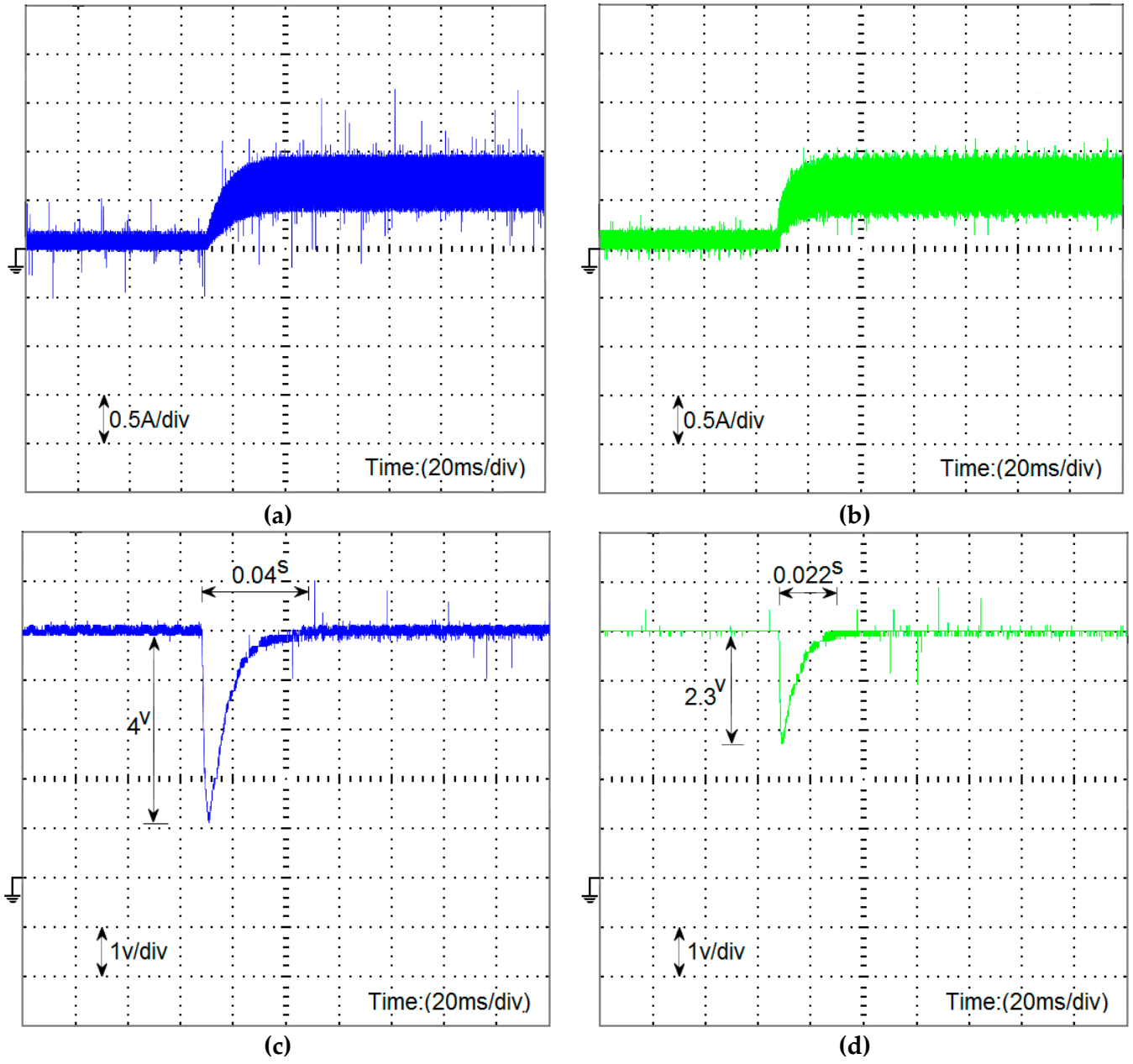

Figure 6. The experimental responses of proposed adaptive SMC and double-loop SMC during the step changes of the converter load (vertical scale is 1 V per square and time scale is 20 ms per square). (**a**) The inductor current of double-loop SMC. (**b**) The inductor current of the proposed adaptive PSMC. (**c**) The output voltage of double-loop SMC. (**d**) The output voltage of the proposed adaptive PSMC.

4.3.2. Experimental Response of the Proposed SMC during Input Voltage Changes

Assuming a 200 Ω resistor as a converter load that leads to a converter operation in discontinuous mode, the response of the proposed PSMC is presented in Figure 7a during the step changes of input voltage from 12 V to 17 V. It is observed that despite large changes in the input voltage, the converter operates stably and tracks the reference output voltage +5 V with zero steady state error.

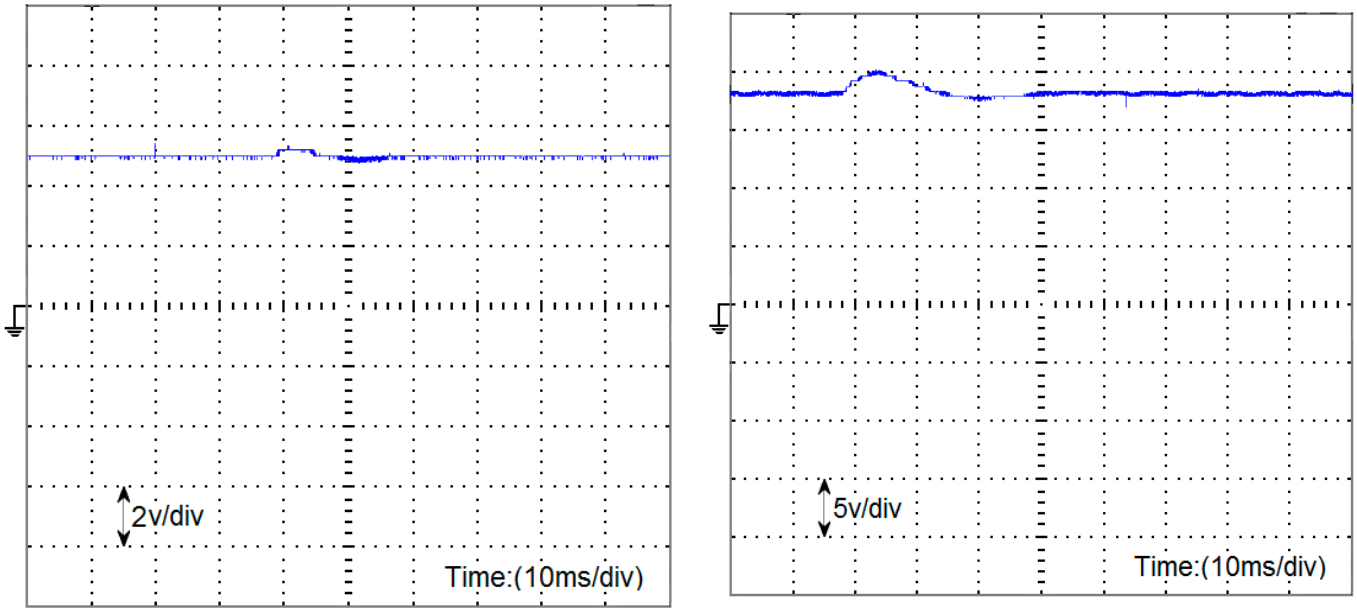

(**a**) (**b**)

Figure 7. Experimental response of the proposed controller during load and line changes. (**a**) Response of the proposed controller during step changes of the input voltage from 12 V to 17 V (vertical scale is 2 V per square and time scale is 10 ms per square). (**b**) The output voltage of the converter during load changes in boost operating mode (vertical scale is 5 V per square and time scale is 10 ms per square).

4.3.3. Experimental Response of Proposed Controller during Load Resistance Changes in Voltage-Boost Operation

In this experiment, to evaluate the response of the system in voltage boost operating, it is assumed that $V_{ref} = 18$ V and the value of the load resistance is stepped from 200 Ω to 100 Ω. In this test, the converter output voltage is shown in Figure 7b. It is observed that the proposed controller is stable against load resistance in voltage boost operation as well.

4.3.4. Experimental Response of the Proposed Controller during the Reference Voltage Changes

Considering the nominal parameters of the converter, responses of the proposed controller and standard double-loop SMC [18] are shown in Figure 8 for stepped changes of the output reference voltage. In this test, the reference voltage is stepped up from +5 V to +15 V. It is seen that the response of the proposed controller is stable in a wide range of output voltage changes and it has a superior dynamic response compared with standard double-loop SMC [18] in terms of response overshoot and settling time.

All tests are performed using $\rho = k = k_I = 200$ as gains of the controller.

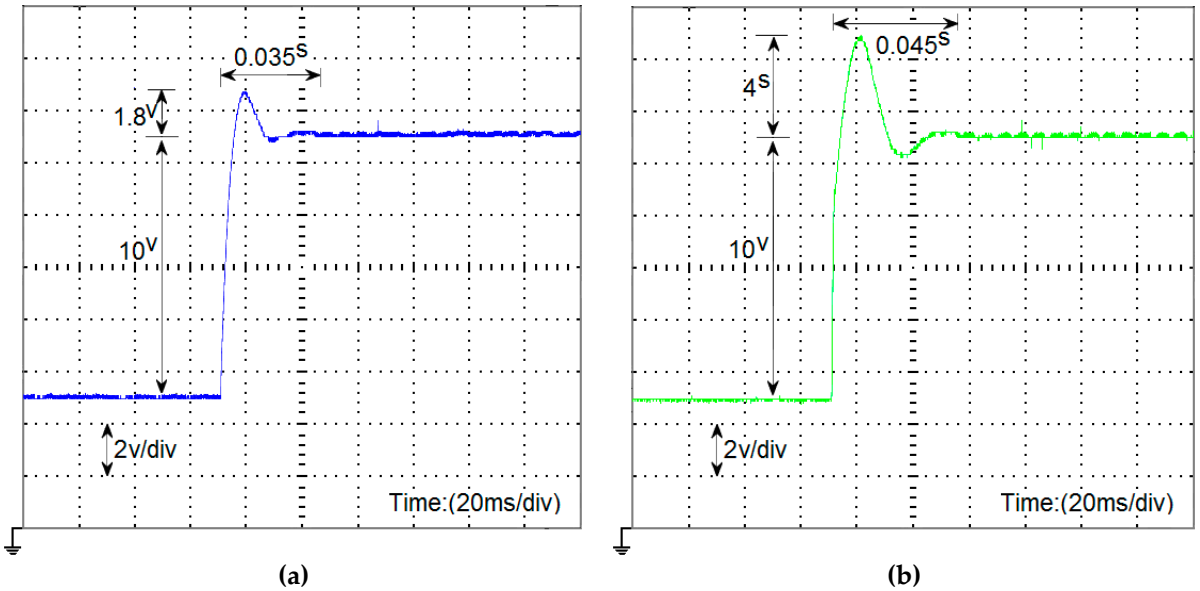

Figure 8. Comparison of the proposed and double-loop controllers during voltage reference changes. (**a**) Output voltage of the proposed adaptive PSMC (vertical scale is 2 V per square and time scale is 20 ms per square). (**b**) Output voltage of the double-loop standard SMC (vertical scale is 2 V per square and time scale is 20 ms per square).

5. Conclusions

To cope with the drawbacks of the two-loop SMC, a novel adaptive partial SMC (PSMC) is presented for closed-loop control of the switch-mode power supplies. Considering the simulation and experimental results, it is shown that the developed PSMC can stabilize the output voltage robustly in wide changes of load resistance and input voltage changes in both discontinuous and continuous modes. Furthermore, to avoid the trial-and-error method during the controller tuning, a systematic approach is developed for the controller gains selection, which guarantees the stable operation of the closed-loop system. It should be noted that the appropriate ranges of controller gains are obtained considering the root locus analysis. To extract the controller, first, a fixed-frequency PSMC is designed for SMPS based on the nominal values of the converter parameters using the equivalent control approach. To simplify the controller in comparison with the conventional SMCs, the partial SMC (PSMC) approach is introduced in this article, which just requires a part of a sliding surface for the controller formulation. The accuracy of the developed PSMC is proved mathematically within the entire range of operation. To improve the robustness of the controller against uncertainties of the model, an adaptive term is added to the designed PSMC. Asymptotical stability of the designed SMC was demonstrated in both discontinuous and continuous modes using Lyapunov stability criteria. Compared to the standard two-loop controller, it is shown that the presented adaptive PSMC has a superior dynamic response in terms of response overshoot and settling time. The performance and accuracy of the proposed method were verified using MATLAB/Simulink simulations as well as the practical results.

Funding: This research received no external funding.

Conflicts of Interest: The authors declare no conflict of interest.

References

1. Mostafa, M.R.; Saad, N.H.; El-sattar, A.A. Tracking the maximum power point of PV array by sliding mode control method. *Ain Shams Eng. J.* **2020**, *11*, 119–131. [CrossRef]
2. Mustafa, G.; Ahmad, F.; Zhang, R.; Haq, E.U.; Hussain, M. Adaptive sliding mode control of buck converter feeding resistive and constant power load in DC icrogrid. *Energy Rep.* **2023**, *9* (Suppl. S1), 1026–1035. [CrossRef]

3. Paul, A.K. Sensorless Robust Speed Controller Design of Pancake Axial Field PMDC Motor. In *IEEE Transactions on Industry Applications*; IEEE: Piscataway, NJ, USA, 2019; Volume 55, pp. 5981–5989.
4. Ali, N.; Liu, Z.; Armghan, H.; Armghan, A. Double integral sliding mode controller for wirelessly charging of fuel cell-battery-super capacitor based hybrid electric vehicle. *J. Energy Storage* **2022**, *51*, 104288. [CrossRef]
5. Salimi, M.; Klumpner, C.; Bozhko, S. Sliding Mode Input Current Control of the Synchronous DC-DC Buck Converter for Electro-Mechanical Actuator Emulation in More Electric Aircrafts. *Energies* **2022**, *15*, 9628. [CrossRef]
6. Wu, L.; Lei, B.; Sun, M. Steady-State Error Band Improvement Using Dead-Beat Terminal Sliding Mode Control. In *IEEE Transactions on Circuits and Systems II: Express Briefs*; IEEE: Piscataway, NJ, USA, 2022; Volume 69, pp. 3590–3594.
7. Xiong, X.; Chu, Y.; Udai, A.D.; Kamal, S.; Jin, S.; Lou, Y. Implicit Discrete-Time Terminal Sliding Mode Control for Second-Order Systems. In *IEEE Transactions on Circuits and Systems II: Express Briefs*; IEEE: Piscataway, NJ, USA, 2021; Volume 68, pp. 2508–2512.
8. Al-Baidhani, H.; Kazimierczuk, M.K. Simplified Double-Integral Sliding-Mode Control of PWM DC-AC Converter with Constant Switching Frequency. *Appl. Sci.* **2022**, *12*, 10312. [CrossRef]
9. Mohammadinodoushan, M.; Abbassi, R.; Jerbi, H.; Ahmed, F.W.; Abdalqadir kh ahmed, H.; Rezvani, A. A new MPPT design using variable step size perturb and observe method for PV system under partially shaded conditions by modified shuffled frog leaping algorithm- SMC controller. *Sustain. Energy Technol. Assess.* **2021**, *45*, 101056. [CrossRef]
10. Asma, C.; Abdelaziz, Z.; Nadia, Z. Dual loop control of DC-DC boost converter based cascade sliding mode control. In Proceedings of the 2017 International Conference on Green Energy Conversion Systems (GECS), Hammamet, Tunisia, 23–25 March 2017; pp. 1–6.
11. Kumar, P.; Ajmeri, M. Comparative Analysis of Different Controlling Techniques of Boost Converter. In Proceedings of the 2022 IEEE 7th International conference for Convergence in Technology (I2CT), Mumbai, India, 7–9 April 2022; pp. 1–6.
12. Dong, C.; Jiang, W.; Xiao, Q.; Li, X.; Jin, Y.; Dragičević, T. Modeling, Analysis, and Adaptive Sliding-Mode Control of a High-Order Buck/Boost DC-DC Converter. In Proceedings of the IECON 2019—45th Annual Conference of the IEEE Industrial Electronics Society, Lisbon, Portugal, 14–17 October 2019; pp. 1844–1849.
13. Saadat, S.A.; Ghamari, S.M.; Mollaee, H. Adaptive backstepping controller design on Buck converter with a novel improved identification method. *IET Control Theory Appl.* **2022**, *16*, 485–495. [CrossRef]
14. Fu, Z.; Wang, Y.; Tao, F.; Si, P. An Adaptive Nonsingular Terminal Sliding Mode Control for Bidirectional DC–DC Converter in Hybrid Energy Storage Systems. *Can. J. Electr. Comput. Eng.* **2020**, *43*, 282–289. [CrossRef]
15. González Montoya, D.; Ortiz Valencia, P.A.; Ramos-Paja, C.A. Fixed-frequency implementation of sliding-mode controllers for photovoltaic systems. *Int. J. Energy Environ. Eng.* **2019**, *10*, 287–305. [CrossRef]
16. Dong, L.; Nguang, S.K. Chapter 5—Sliding mode control for multiagent systems with continuously switching topologies based on polytopic model. In *Consensus Tracking of Multi-Agent Systems with Switching Topologies*; Emerging Methodologies and Applications in Modelling; Dong, L., Nguang, S.K., Eds.; Academic Press: Cambridge, MA, USA, 2020; pp. 87–105.
17. Murthy, A.; Badawy, M. State space averaging model of a dual stage converter in discontinuous conduction mode. In Proceedings of the 2017 IEEE 18th Workshop on Control and Modeling for Power Electronics (COMPEL), Stanford, CA, USA, 9–12 July 2017; pp. 1–7.
18. Chen, Z. Double loop control of buck-boost converters for wide range of load resistance and reference voltage. *IET Control Theory Appl.* **2012**, *6*, 900–910. [CrossRef]